

# Self-supervised asymmetric deep hashing with margin-scalable constraint for image retrieval

Zhengyang Yu<sup>a,1</sup>, Zhihao Dou<sup>a,2</sup>, Erwin M. Bakker<sup>b</sup> and Song Wu<sup>a,\*</sup>

<sup>a</sup>College of Computer and Information Science, Southwest University, Chongqing, China

<sup>b</sup>LIACS Media Lab, Leiden University, Leiden, Netherlands

## ARTICLE INFO

### Keywords:

Large-scale image retrieval  
Asymmetric hashing  
Self-supervised learning

## ABSTRACT

Due to its effectivity and efficiency, image retrieval based on deep hashing approaches is widely used especially for large-scale visual search. However, many existing deep hashing methods inadequately utilize label information as guidance for feature learning networks without more advanced exploration of the semantic space. Besides the similarity correlations in the Hamming space are not fully discovered and embedded into hash codes, by which the retrieval quality is diminished with inefficient preservation of pairwise correlations and multi-label semantics. To cope with these problems, we propose a novel self-supervised asymmetric deep hashing method with a margin-scalable constraint(SADH) approach for image retrieval. SADH implements a self-supervised network to preserve semantic information in a semantic feature map and a semantic code map for the semantics of the given dataset, which efficiently and precisely guides a feature learning network to preserve multi-label semantic information using an asymmetric learning strategy. Moreover, for the feature learning part, by further exploiting semantic maps, a new margin-scalable constraint is employed for both highly-accurate construction of pairwise correlations in the hamming space and a more discriminative hash code representation. Extensive empirical research on three benchmark datasets validates the proposed method and shows it outperforms several state-of-the-art approaches. The source codes URL of our SADH is: <http://github.com/SWU-CS-MediaLab/SADH>.

## 1. Introduction

The amount of image and video data in social networks and search engines are growing at an alarming rate. In order to effectively search large-scale high dimensional image data, researchers proposed the Approximate Nearest Neighbor (ANN)[1, 2]. As an ANN algorithm, the hash algorithm is widely used in the field of large-scale image retrieval. It maps high-dimensional content features of pictures into Hamming space (binary space) to generate a low-dimensional hash sequence[1, 2].


Hash algorithms can be broadly divided into data-dependent methods and data-independent methods[3] schemes. The most basic but representative data independent method is Locality Sensitive Hashing LSH[1], which generates an embedding through random projections. However, these methods all require long binary codes to achieve accuracy, which is not suitable for the processing of large-scale visual data. Recent research priorities have shifted to data-dependent approaches that can generate compact binary codes by learning from large amounts of data and information. This type of method embeds high-dimensional data into the Hamming space and performs bitwise operations to find similar objects. Recent data-dependent works such as ITQ, KMH, KSH, BRE, SH, MLH and Hamming Distance Metric Learning[2, 4–9] have shown better retrieval accuracy using smaller hash code lengths.

Although the above data-dependent hashing methods have certainly succeeded to some extent. Their performance

unexceptionally rely on the quality of hand crafted features, meanwhile the feature learning procedure cannot be optimized with hash code learning simultaneously, thereby limiting the retrieval accuracy of learned binary code. Recently, the deep-learning-based hashing methods have shown superior performance by combining the powerful feature extraction of deep learning[10–15]. Nevertheless, most of these approaches simply employ classification constraints with semantic labels and contrastive loss with pairwise labels as guidance during deep feature learning and hash code generation, which seemingly leads to two problems. Firstly, such supervising mode may be beneficial for the extraction of deep semantic features, whereas the quality of the generated hash code is relatively neglected. Secondly, it is also noteworthy that in many datasets such as NUS-WIDE[16] and MIRFlickr-25K[17], an image is annotated with multi-labeled semantics, where the item pairs that share more relevant semantics should be generating hashing codes that are closer in the hamming space comparing to those with less semantic similarity, thus it is crucial to build a more advanced correlation mechanism to store more advanced similarity information between image pairs and to generate discriminative hash codes with rich multi-label semantic information.

To tackle the mentioned flaws, we proposed a novel self-supervised asymmetric deep hashing with margin-scalable constraint(SADH) approach to improve the accuracy and efficiency of image retrieval. Despite the feature learning strategy with direct semantic supervision and similarity constraints in many deep hashing methods, we proposed a self-supervised network to generate a class-based semantic code map and a semantic feature map with rich semantic information, which can asymmetrically supervise the feature learning net-

\*Corresponding author

 [songwuswu@swu.edu.cn](mailto:songwuswu@swu.edu.cn) (S. Wu)

ORCID(s):

work. Meanwhile, a new margin-scalable constraint is proposed based on semantic maps generated by self-supervised network to build highly-precise pairwise correlations which in turn effectively cluster the high-dimensional feature and hash code of similar item pairs, and to separate the dissimilar ones simultaneously. The main contributions of this paper are as follows:

- 1) Aiming to preserve more semantic information in the feature learning network. An asymmetric hashing method is proposed with the generation of a hash code map and a semantic feature map by a self-supervised network. To the best of our knowledge, it is the first work to utilize an asymmetric learning strategy for the exploration of semantic information for hash function learning for large-scale visual search.
- 2) Based upon the generated semantic maps. A new margin-scalable constraint is proposed in the pursuit of discriminative hash code representation of feature learning network with the exploration of highly-accurate pairwise correlations and abundant multi-label semantics.
- 3) The experimental results of SADH on CIFAR-10, NUS-WIDE and MIRFlickr-25K outperforms several state-of-the-art image retrieval hashing methods.

## 2. Related work

### 2.1. Non-deep hashing methods

The unsupervised hashing methods[2, 18–23], including Isotropic hashing[24], Spectral Hashing (SH)[7], PCA-Iterative Quantization (ITQ) [2], etc, attempt to map the original features to the Hamming space while using the unlabeled data to preserve the similarity relationship between the original features. However, unsupervised hashing methods may lose rich semantic information available in image tags. To handle more complex semantic similarities, supervised approaches has been proposed to exploit tag information. Supervised hashing with kernel (KSH) [5] and supervised discrete hashing (SDH) [24] generate binary hash codes by minimizing the Hamming distance through similar data point pairs. Distortion Minimization Hashing (DMS)[8], Minimum Loss Hashing (MLH)[25] and Order Retention Hash (OPH)[26] learn to disperse by minimizing a triplet loss based on pairs of similar pairs. Although the above hashing methods have certainly succeeded to some extent, they all use hand-crafted features that do not fully capture the semantic information and do not combine feature learning and hash function learning into one state, thereby causing suboptimal problem in learning binary codes.

### 2.2. Deep hashing methods

Recently, the deep learning-based hashing methods have shown superior performance by exploiting the powerful feature extraction of deep learning[25, 27–37]. In particular, Convolutional Neural Network Hash (CNNH) [38] is a two-stage hashing method that learns hash codes and deep hash

functions for image retrieval, respectively. DNNH [11] improved [38] by simultaneous feature learning and hash code learning, similarly DSPH[10] performs joint hash code learning and feature learning with pairwise labels. HashNet[13] equip the deep network with sign as activation function to directly optimize the hashing function. DDSH[39] utilizes semantic labels to directly supervise both hash code learning and deep feature learning. Both pairwise label information and classification supervision are used in DSDH[40] to learn hash codes in a single framework. Although these methods have obtained satisfactory retrieval performance, they ignore to construct more precise pairwise correlations between pairs of hash codes and deep features, which may downgrade retrieval accuracy. Besides, they mostly hardness supervised information to directly guide the feature learning procedure of deep networks, which may suffer substantial loss of semantic information.

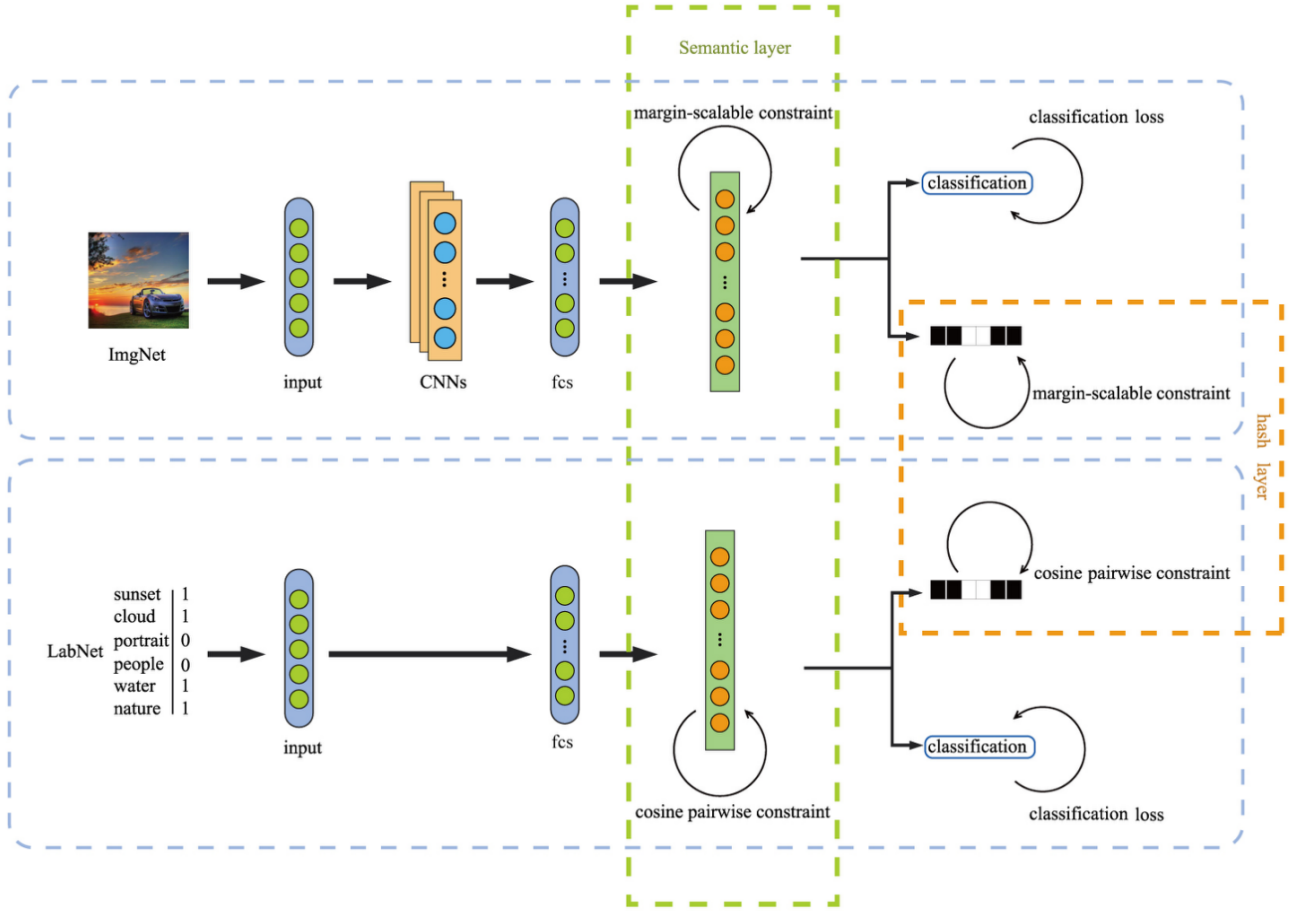
To solve this limitation, some methods have been proposed to further enrich the semantic information of hash codes in addition to direct semantic supervision, DSEH and AD-SQ[41, 42] utilizes self-supervised networks to capture rich pairwise semantic information to guide the feature learning network at both the semantic level and the hash codes level, thus enriching semantic information and pairwise correlation in hash codes. In comparison to [41, 42] our work improves the guidance mechanism of self-supervised network on feature learning network effectively and is more semantic-targeted with an asymmetric learning strategy. Moreover, the generated semantic codes are further exploited to identify scalable margins for a pairwise contrastive-form constraint for higher-level pairwise correlations and highly-discriminative hash code representations.

### 2.3. Asymmetric hashing methods

Asymmetric hashing methods[3, 19, 42, 43] have recently become very active area of research. In ADSH [19], query points and database points are treated asymmetrically, with only query points being engaged in the stage of updating deep network parameters, while the hash codes for database are directly learned as independent parameters, the hash codes generated by the query and database are correlated through asymmetric pairwise constraints, such that the dataset points can be efficiently utilized during the hash function learning procedure. AGAH[44] adopts an asymmetric discrete loss to ensure multi-label semantic preservation in cross modality hashing retrieval. To the best of our knowledge, our work is the first attempt to exploit an asymmetric learning strategy in the guidance of a self-supervised network on a feature learning network in the pursuit of comprehensive and efficient semantic preservation.

## 3. The proposed method

We elaborate our proposed SADH in details. Firstly, the problem formulation for hash function learning is presented. Afterwards, each module as well as the optimization strategy in the self-supervised network (namely LabNet) and feature learning network (namely ImgNet) are explicitly



**Figure 1:** The overall framework of ImgNet and LabNet as used in our proposed SADH, ImgNet is comprised of a deep convolutional layers(CNNs) for deep image representations, while LabNet is an end-to-end fully connected deep neural network which abstracts semantic features from one-hot annotations as inputs. Both networks embeds deep features into a semantic space through a semantic layer, and independently obtain classification outputs and binary codes using multi-task learning framework. The asymmetric guidance mechanism between networks is further illustrated in Fig.2.

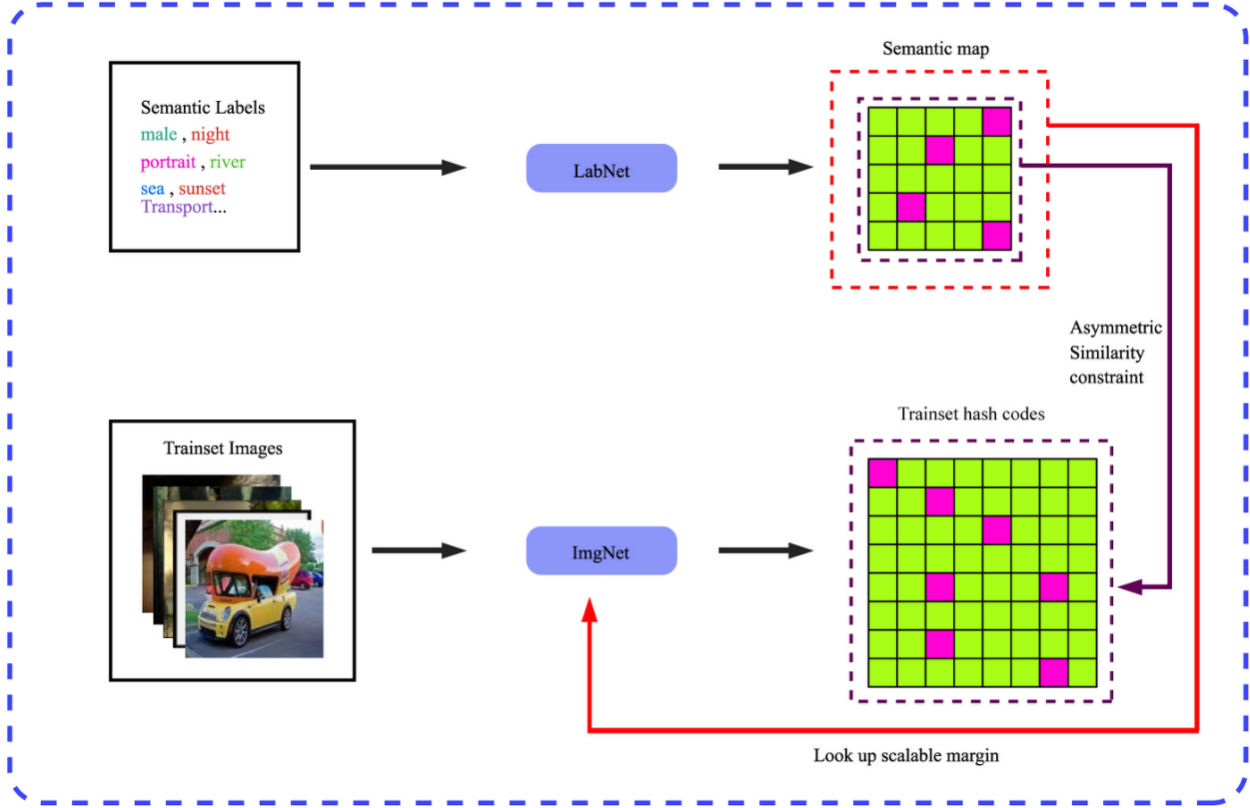
described. As can be seen in the overall framework Fig.1, SADH consists of two networks, where LabNet is a deep fully-connected network for semantic preservation with one-hot labels as inputs. ImgNet is a convolutional neural network which maps input images into binary hash codes, with both deep features (generated by semantic layer) and hash codes (generated by hash layer) under asymmetric guidance of LabNet as shown in Fig.2.

### 3.1. Problem definition

First the notations used in the rest of the paper are introduced. In an image retrieval problem, let  $O = \{o_l\}_{l=1}^m$  denote a dataset with  $m$  instances, and  $o_l = (v_l, l_l)$  where  $v_l \in \mathbb{R}^{1 \times d_v}$  is the original image feature from the  $l$ -th sample. Assuming that there are  $C$  classes in this dataset,  $o_l$  will be annotated with multi-label semantic  $l_l = [l_{l1}, \dots, l_{lc}]$ , where  $l_{ij} = 1$  indicates that  $o_l$  belongs to the  $j$ -th class, and  $l_{ij} = 0$  if not. The image-feature matrix is noted as  $V$ , and the label matrix as  $L$  for all instances. The pairwise multi-label similarity matrix  $S$  is used to describe semantic similarities

between each of the two instances, where  $S_{i,j} = 1$  means that  $O_i$  is semantically similar to  $O_j$ , otherwise  $S_{i,j} = 0$ . In a multi-label setting, two instances ( $O_i$  and  $O_j$ ) are annotated by multiple labels. Thus, we define  $S_{i,j} = 1$ , if  $O_i$  and  $O_j$  share at least one label, otherwise  $S_{i,j} = 0$ . The main goal in deep hashing retrieval is to identify a nonlinear hash function, i.e.,  $H : o \rightarrow h \in \{-1, 1\}^K$ , where  $K$  is the length of each hash codes, to encode each item  $o_l$  into a  $K$ -bit hash code  $H_i \in \{-1, 1\}$ , whereby the correlation of all item pairs are maintained. The similarity between a hash code pair  $H_i, H_j$  are evaluated by their Hamming distance  $dis_H(H_i, H_j)$ , which might be a challenging and costly calculation [45]. The inner-product  $\langle H_i, H_j \rangle$  can be used as a surrogate which relates to hamming distance as follows:

$$dis_H = \frac{l}{2} (K - \langle H_i, H_j \rangle). \quad (1)$$



**Figure 2:** Overview of the proposed asymmetric guidance scheme between LabNet and ImgNet in our SADH. A group of hash codes and their related deep features related to the semantics in the given dataset (semantic maps) is obtained by the converged LabNet. These asymmetrically guide ImgNet, which is fed into images of the entire trainset. The semantic maps are further exploited to define scalable margins in the pairwise constraint of ImgNet.

### 3.2. Self-supervised network

To enrich the semantic information in generated hash codes, we designed a fully-connected LabNet to leverage abundant semantic correlations from multi-label annotations as a guidance of the further feature learning process of ImgNet.

LabNet extracts high-dimensional semantic features through fully-connected layers with multi-label annotations as inputs (i.e.,  $H_i^l = f^l(I_i, \theta^l)$ ), where  $f^l$  is the nonlinear hash function for LabNet, while  $\theta^l$  denotes the parameters for LabNet. With a sign function the learned  $H^l$  can be discretized into binary codes:

$$B^l = \text{sign}(H^l) \in \{-1, 1\}^K. \quad (2)$$

For more advanced preservation of semantic information especially in multi-label scenarios, the high-dimensional semantic features  $F^l = [F_1^l, \dots, F_n^l]$  of LabNet are also exploited to supervise the semantic learning of ImgNet.

#### 3.2.1. Cosine-distance-based similarity evaluation

In Hamming space, the similarity of two hash codes  $H_i$ ,  $H_j$  can be defined by the Hamming distance  $\text{dist}_H(*, *)$ . To

preserve the similarity of item pairs, whereby similar pairs are clustered and dissimilar pairs scattered, a similarity loss function of LabNet is defined as follows:

$$J_s = \sum_{i,j=1}^n (s_{i,j} \text{dis}_H(H_i, H_j) + (1 - s_{i,j}) \max(m - \text{dis}_H(H_i, H_j), 0)) \quad (3)$$

Where  $J_s$  denotes the similarity loss function, by which the similarity of two generated hash codes  $H_i$  and  $H_j$  can be preserved.  $\text{dis}_H(H_i, H_j)$  represents the Hamming distance between  $H_i$  and  $H_j$ . To avoid the collapsed scenario[46], a contrastive form of loss function is applied with a margin parameter  $m$ , with which the hamming distance of generated hash code pairs are expected to be less than  $m$ . With the mentioned relationship (1) between Hamming distance and inner-product, the similarity loss can be redefined as:

$$J_s = \sum_{i,j=1}^n \frac{1}{2} (s_{i,j} \max(m - \langle H_i, H_j \rangle, 0) + (1 - s_{i,j}) \max(m + \langle H_i, H_j \rangle, 0)) \quad (4)$$



Where the margin parameter induce the inner-product of dissimilar pairs to be less than  $-m$ , while that of similar ones to be larger than  $m$ . For enhancement of similarity preservation, we expect the similarity constraint to be extended by ensuring the discrimination of deep semantic features. However because of the difference between the distributions of features from Labnet and Imgnet, the inner-product  $\langle \cdot, \cdot \rangle \in (-\infty, \infty)$  will no longer be a plausible choice for the similarity evaluation between the semantic features of the two networks. As the choice of margin parameter  $m$  is ambiguous. one way to resolve this flaw is to equip the two networks with the same activate function, for example a sigmoid or tanh, at the output of the semantic layer to limit the scale of output features to a fixed range, nevertheless we expect both of the networks to maintain their own scale of deep features. Considering the fact that hash codes are discretized to either -1 or 1 at each bit, meanwhile all generated hash codes have the same length  $K$ , therefore in the similarity evaluation in Hamming space, we choose to focus more on the angles between hash codes, instead of the absolute distance between them. Hence we adopt the cosine distance  $\cos(\cdot, \cdot)$  as a replacement:

$$\cos(H_i, H_j) = \frac{\langle H_i, H_j \rangle}{\|H_i\| \|H_j\|} \quad (5)$$

Where  $\cos(H_i, H_j) \in (-1, 1)$ . Although pairwise label information is adopted to store the semantic similarity of hash codes, the label information is not fully exploit. Thus Labnet will further exploit semantic information through classification task and hashing task jointly. Many recent works directly map the learned binary codes into classification predictions by using a linear classifier[40, 41]. To prevent the interference between the classification stream and hashing stream, and to avoid the classification performance being too sensitive to the length of hash codes, both the hash layer and classification layer are performed as output layers of Labnet under a multi-task learning scheme[47, 48].

The final object function of LabNet can be formulated as:

$$\begin{aligned} & \min_{B^l, \theta^l, \hat{L}^l} J_{Lab} \\ & = \alpha J_1 + \lambda J_2 + \eta J_3 + \beta J_4 \\ & = \alpha \sum_{i,j=1}^n \frac{1}{2} S_{i,j} \max(m - \Delta_{i,j}^l, 0) + \frac{1}{2} (1 - S_{i,j}) \max(m + \Delta_{i,j}^l, 0) \\ & + \lambda \sum_{i,j=1}^n \frac{1}{2} S_{i,j} \max(m - \Gamma_{i,j}^l, 0) + \frac{1}{2} (1 - S_{i,j}) \max(m + \Gamma_{i,j}^l, 0) \\ & + \eta \|\hat{L}^l - L\|_2^2 + \beta \|H^l - B^l\|_2^2 \end{aligned} \quad (6)$$

Where the margin constant  $m \in (0, 1)$ .  $J_1$  and  $J_2$  are the similarity loss for the learned semantic features and hash codes respectively with  $\Delta_{i,j}^l = \cos(F_i^l, F_j^l)$ ,  $\Gamma_{i,j}^l = \cos(H_i^l, H_j^l)$ . The classification loss  $J_3$  calculates the difference between input labels and predicted labels.  $J_4$  is the quantization loss for the discretization of learned hash codes.

### 3.2.2. Asymmetric learning strategy

In many self-supervised methods [26, 49], the self-supervised network is trained with a feature learning network simultaneously, with one image input into Imgnet and it's label input into Labnet. Under such mechanism, two networks will generate the same number of hash codes, where one supervises the other by a pairwise similarity constraint. In this paper, we focus on optimizing such form of guidance in a more efficient and semantic-targeted way. Inspired by ADSH where query points and database points are treated asymmetrically with a deep hash function learned for only the query points. As illustrated in Fig.2, we use the converged LabNet to generate semantic features and hash codes with only binary representations that correspond to each semantic label as inputs, which gives a hash code map  $U = \{u_i\}_{i=1}^C$  where  $u_i \in [-1, 1]$  and a corresponding semantic feature map  $Q = \{q_i\}_{i=1}^C$ , where  $C$  is the total number of classes. Also with the adoption of cosine similarity, the scale of semantic features is not constrained.

### 3.3. Feature learning network

We apply an end-to-end convolutional neural network for image feature learning, which can extract and embed deep visual features from images into high dimensional semantic features and simultaneously project them into representations for multi-label classification task and discrete hash codes for metric learning task. Similar to Labnet, we add extra output layer and hash layer to embed the high-dimensional semantic features into  $K$ -dimensional hash codes and  $C$ -dimensional classification predictions using multi-task learning framework. The generation of both the semantic features and hash codes of ImgNet will be constrained by the semantic maps  $U$  and  $Q$  generated in LabNet by an asymmetric learning strategy, using the following asymmetric discrete loss:

$$\begin{aligned} J_s = \sum_{i=1}^n \sum_{j=1}^c \frac{1}{2} (s_{i,j} \max(m - \cos(H_i, u_j), 0) \\ + (1 - s_{i,j}) \max(m + \cos(H_i, u_j), 0)) \end{aligned} \quad (7)$$

where  $s_{i,j}$  is an asymmetric affinity matrix.

#### 3.3.1. Margin-scalable constraint

In most contrastive forms of pairwise or triplet similarity constraints used in deep hash methods[19, 50, 51], the choice of the margin parameter mainly relies on manual tuning. Subsequently for all the item pairs, the margin parameter is used as a fixed constant, In this way, it can be hypothesized that the performance of hash learning will be highly sensitive to the choice of margin parameter, which will be demonstrated later in 4.3.2. Also in multi-label scenarios, the expected margin parameter for item pairs that share more semantic similarities should be larger than pairs with less semantic similarities. Thus setting a single fixed margin value may downgrade the storage of similarity information. To optimize the selection of margin value, we propose a margin-scalable constraint based on the semantic maps generated by

Labnet. Specifically for two hash codes  $H_i^v$  and  $H_j^v$  generated by ImgNet, a pair of hash codes  $q_{H_i^v}$  and  $q_{H_j^v}$  are represented by looking up the semantic code map  $Q$  with respect to their semantic labels will be assigned to them. The scalable margin  $M_{H_i, H_j}$  for  $H_i^v$  and  $H_j^v$  is calculated by:

$$M_{H_i, H_j} = \max\left(0, \cos\left(q_{H_i^v}, q_{H_j^v}\right)\right) \quad (8)$$

As  $\cos\left(q_{H_i^v}, q_{H_j^v}\right) \in (-1, 1)$ , a positive cosine distance between item pairs in the semantic code map will be assigned to similar item pairs and will be used by ImgNet to calculate their scalable margin, while the negative cosine distances will scale the margin to 0. This is due to the nature of multi-label tasks, where the ‘dissimilar’ situation only refers to item pairs with a zero identical label. While for a pair of similar items, the number of shared labels may come from a wide range. Thus, in the pairwise similarity preservation, dissimilar items are given a weaker constraint, whereas the similar pairs are constrained in a more precise and strong way, considering similarity differences between specific items pairs.

Using Equations (7) and (8), the final object function of ImgNet can be formulated as:

$$\begin{aligned} & \min_{B^v, \theta^v, \hat{L}^v} J_{\text{Img}} \\ & = \alpha J_1 + \lambda J_2 + \gamma J_3 + \mu J_4 + \eta J_5 + \beta J_6 \\ & = \alpha \sum_{i,j=1}^n \frac{1}{2} \left( S_{i,j} \max\left(M_{F_i, F_j} - \Delta_{i,j}^v, 0\right) \right. \\ & \quad \left. + (1 - S_{i,j}) \max\left(\Delta_{i,j}^v - M_{F_i, F_j}, 0\right) \right) \\ & \quad + \lambda \sum_{i,j=1}^n \frac{1}{2} \left( S_{i,j} \max\left(M_{H_i, H_j} - \Gamma_{i,j}^v, 0\right) \right. \\ & \quad \left. + (1 - S_{i,j}) \max\left(\Gamma_{i,j}^v - M_{H_i, H_j}, 0\right) \right) \quad (9) \\ & \quad + \gamma \sum_{i=1}^n \sum_{j=1}^c \frac{1}{2} \left( S_{i,j} \max\left(M_{F_i, q_j} - \Phi_{i,j}, 0\right) \right. \\ & \quad \left. + (1 - S_{i,j}) \max\left(\Phi_{i,j} - M_{F_i, q_j}, 0\right) \right) \\ & \quad + \mu \sum_{i=1}^n \sum_{j=1}^c \frac{1}{2} \left( S_{i,j} \max\left(M_{H_i, u_j} - \Psi_{i,j}, 0\right) \right. \\ & \quad \left. + (1 - S_{i,j}) \max\left(\Psi_{i,j} - M_{H_i, u_j}, 0\right) \right) \\ & \quad + \eta \|\hat{L}^v - L\|_2^2 + \beta \|H^v - B^v\|_2^2 \end{aligned}$$

where  $J_1$  and  $J_2$  are margin scalable losses for generated semantic features  $F$  and hash codes  $H$ , with  $\Delta_{i,j}^v = \cos\left(F_i^v, F_j^v\right)$ ,  $\Gamma_{i,j}^v = \cos\left(H_i^v, H_j^v\right)$ .  $J_3$  and  $J_4$  asymmetric losses for hash codes and semantic. Features  $\Phi_{i,j} = \cos\left(F_i^v, q_j\right)$ ,  $\Psi_{i,j} = \cos\left(H_i^v, u_j\right)$ .  $J_5$  and  $J_6$  are classification loss and quantization loss similarly defined in LabNet.

### 3.4. Optimization

It is noteworthy to mention that, the ImgNet is trained after the convergence of LabNet is obtained. First we iteratively optimize the objective function (6) by exploring multi-label information to learn  $\theta^l$ ,  $H^l$  and  $\hat{L}^l$ . With the finally trained LabNet we obtain  $U$  and  $V$ . Then the parameters of LabNet will be fixed, and  $L_{\text{img}}$  will be optimized through  $\theta^v$ ,  $H^v$  and  $\hat{L}^v$  with the guidance of  $U$  and  $Q$ . Finally, we obtain binary hash codes  $B = \text{sign}(H^v)$ . The entire learning algorithm is summarized in Algorithm 1 in more detail.

#### 3.4.1. Optimization of LabNet

The gradient of  $J_{\text{Lab}}$  w.r.t each Hash code  $H_i^l$  in sampled mini-batch is

$$\frac{\partial J_{\text{Lab}}}{\partial H_i^l} = \begin{cases} \sum_{j=1}^n \frac{\lambda}{2} \left( m - \frac{H_j^l}{\|H_i^l\| \|H_j^l\|} + \frac{H_i^l \Gamma_{i,j}^l}{\|H_i^l\|_2^2} \right) + 2\beta (H_i^l - B_i^l) & \text{if } s_{i,j} = 1 \text{ and } \Gamma_{i,j}^l < m \\ \sum_{j=1}^n \frac{\lambda}{2} \left( m + \frac{H_j^l}{\|H_i^l\| \|H_j^l\|} - \frac{H_i^l \Gamma_{i,j}^l}{\|H_i^l\|_2^2} \right) + 2\beta (H_i^l - B_i^l) & \text{if } s_{i,j} = 0 \text{ and } \Gamma_{i,j}^l > -m \end{cases} \quad (10)$$

$\frac{\partial J_{\text{Lab}}}{\partial F_j^l}$  can be obtained similarly,  $\frac{\partial J_{\text{Lab}}}{\partial \theta^l}$  can be computed by using the chain rule, then  $\theta^l$  can be updated for each iteration using Adam with back propagation.

#### 3.4.2. Optimization of ImgNet

The gradient of  $J_{\text{Img}}$  w.r.t each Hash code  $H_i^v$  in sampled mini-batch is

$$\frac{\partial J_{\text{Img}}}{\partial H_i^v} = \lambda \frac{\partial J_2}{\partial H_i^v} + \mu \frac{\partial J_4}{\partial H_i^v} + \beta \frac{\partial J_6}{\partial H_i^v} \quad (11)$$

Where

$$\frac{\partial J_2}{\partial H_i^v} = \begin{cases} \sum_{j=1}^n \frac{1}{2} \left( M_{H_i, H_j} - \frac{H_j^v}{\|H_i^v\| \|H_j^v\|} + \frac{H_i^v \Gamma_{i,j}^v}{\|H_i^v\|_2^2} \right) & \text{if } s_{i,j} = 1 \text{ and } M_{H_i, H_j} > \Gamma_{i,j}^v \\ \sum_{j=1}^n \frac{1}{2} \left( \frac{H_i^v \Gamma_{i,j}^v}{\|H_i^v\|_2^2} - \frac{H_j^v}{\|H_i^v\| \|H_j^v\|} - M_{H_i, H_j} \right) & \text{if } s_{i,j} = 0 \text{ and } M_{H_i, H_j} > \Gamma_{i,j}^v \end{cases}$$

$\frac{\partial J_6}{\partial H_i^v} = 2(H_i^l - B_i^l)$ , the calculation of  $\frac{\partial J_4}{\partial H_i^v}$  resembles  $\frac{\partial J_2}{\partial H_i^v}$ ,  $\frac{\partial J_2}{\partial F_i^v}$ ,  $\frac{\partial J_{\text{Img}}}{\partial F_i^v}$  can be obtained similarly to  $\frac{\partial J_{\text{Img}}}{\partial H_i^v}$ ,  $\frac{\partial J_{\text{Img}}}{\partial \theta^v}$  can be computed by using the chain rule, then  $\theta^v$  can be updated for each iteration using SGD with back propagation.

**Algorithm 1** The learning algorithm of our SADH**Initialization:**

Image set  $V$ , Label set  $L$

**Output:**

semantic feature map  $V$ , and semantic code map  $Q$ , parameters  $\theta^v$  for ImgNet,

Optimal code matrix for ImgNet  $B^v$

**Initialization:**

Initialize network parameters  $\theta^l$  and  $\theta^v$

Hyper-parameters:  $\alpha, \lambda, \gamma, \mu, \eta, \beta, m$

Mini-batch size  $M$ , learning rate:  $lr$

maximum iteration numbers  $t^l, t^v$

**Stage1:** Hash learning for the self-supervised network (LabNet)**for**  $t^l$  iteration **do**

Calculate derivative using formula (10)

Update  $\theta^l$  by using Adam and back propagation

**end for**

Update semantic feature map  $Q$  and semantic code map  $U$  by Labnet for each semantic as input

**Stage2:** Hash learning for the feature learning network (ImgNet)**for**  $t^v$  iteration **do**

Calculate derivative using formula (11)

Update  $\theta^v$  by using SGD and back propagation

**end for**

Update the parameter  $B^v$  by  $B^v = \text{sign}(H^v)$

## 4. Experiments and analysis

In this section, we conducted extensive experiments to verify three main issues of our proposed SADH method: (1) To illustrate the retrieval performance of SADH compared to existing state-of-the-art methods. (2) To evaluate the improvements of efficiency in our method compared to other methods. (3) To verify the effectiveness of different modules proposed in our method.

### 4.1. Datasets and experimental settings

The evaluation is based on three mainstream image retrieval datasets: CIFAR-10[52], NUS-WIDE[16] and MIRFlickr-25K[17].

**CIFAR-10:** CIFAR-10 contains 60,000 images with a resolution of  $32 \times 32$ . These images are divided into 10 different categories, each with 6,000 images. In the CIFAR-10 experiments, following[53], we select 100 images per category as testing set(a total of 1000) and query set, the remaining as database(a total of 59000), 500 images per category are selected from the database as a training set(a total of 5000).

**NUS-WIDE:** NUS-WIDE contains 269,648 images. This data set is a multi-label image set with 81 ground truth concepts. Following a similar protocol as in [40, 53], we use the subset of 195834 images which are annotated by the 21 most frequent classes (each category contains at least 5,000 images). Among them, 100 images and 500 images are randomly selected in each class as the query set (2100 in total)

and the training set (10500 in total), respectively. The remaining 193734 images are selected as database. We specify that when two images have at least one identical label, the two images are considered similar, otherwise the two images are regarded as dissimilar samples.

**MIRFlickr-25K:** The MIRFlickr25K dataset consists of 25,000 images collected from the Flickr website. Each instance is annotated by one or more labels selected from 38 categories. We randomly selected 1,000 images for the query set, 4,000 images for the training set and the remaining images as the retrieval database. Similar to NUS-WIDE, two images that share at least one identical concept are considered similar, otherwise they are dissimilar.

We compare our proposed SADH with several state-of-the-art approaches including LSH [1], SH [7], ITQ [2], LFH [54], DSDH [40], HashNet [13], DPSH [10], DBDH [55], CSQ [56] and DSEH [41]. These methods are briefly introduced as follows:

1. Locality-Sensitive Hashing (LSH) [1] is a data-independent hashing method that employs random projections as hash function.

2. Spectral Hashing (SH) [7] is a special method which transfers the original problem of finding the best hash codes for a given dataset into the task of graph partitioning.

3. Iterative quantization (ITQ) [2] is a classical unsupervised hashing method. It projects data points into a low dimensional space by using principal component analysis (PCA), then minimize the quantization error for hash code learning.

4. Latent Factor Hashing (LFH) [54] is a supervised method based on latent hashing models with convergence guarantee and linear-time variant.

5. Deep Supervised Discrete Hashing (DSDH) [40] is the first supervised deep hashing method that simultaneously utilize both semantic labels and pairwise supervised information, the hash layer in DSDH is constrained to be binary codes.

6. HashNet [13] is a supervised deep architecture for hash code learning, which includes a smooth activation function to resolve the ill-posed gradient problem during training.

7. Deep pairwise-supervised hashing (DPSH) [10] is a representative deep supervised hashing method that jointly performs feature learning and hash code learning for pairwise application.

8. Deep balanced discrete hashing for image retrieval (DBDH) [55] is a recent supervised deep hashing method which uses a straight-through estimator to actualize discrete gradient propagation.

9. Central Similarity Quantization for Efficient Image and Video Retrieval (CSQ) [56] defines the correlation of hash codes through a global similarity metric, to identify a common center for each hash code pairs.

10. Deep Joint Semantic-Embedding Hashing (DSEH) [41] is a supervised deep hashing method that employs a self-supervised network to capture abundant semantic information as guidance of a feature learning network.

Among the above approaches, LSH[1], SH[7], ITQ[2], LFH [54] are non-deep hashing methods, for these methods, 4096-dimensional deep features extracted from Alexnet [27] are utilized for two datasets: NUS-WIDE and CIFAR-10 as inputs. The other six baselines (i.e., DSDH, HashNet, DPSH, DBDH and DSEH) are deep hashing methods, for which images on three dataset (i.e., NUS-WIDE, CIFAR-10 and MIRFlickr-25k) are resized to  $224 \times 224$  and used as inputs. LSH, SH, ITQ, LFH, DSDH, HashNet and DPSH are carefully carried out based on the source codes provided by the authors, while for the rest of the methods, they are carefully implemented by ourselves using parameters as suggested in the original papers.

We evaluate the retrieval quality by three widely used evaluating metrics: Mean Average Precision (MAP), Precision-Recall curve, and Precision curve with the number of top returned results as variable (topK-Precision).

Specifically, given a query instance  $q$ , the Average Precision (AP) is given by:

$$AP(q) = \frac{1}{n_q} \sum_{i=1}^{n_{database}} P_{q_i} I(i)$$

Where  $n_{database}$  is the total number of instances in the database,  $n_q$  is the number of similar samples,  $P_{q_i}$  is the probability of instances of retrieval results being similar to the query instance at cut-off  $i$ , And  $I(i)$  is the indicator function that indicates the  $i$ -th retrieval instance  $I$  is similar to query image to  $q$ , if  $I(i) = 1$ , and  $I(i) = 0$  otherwise.

The larger the MAP is, the better the retrieval performance. Since NUS-WIDE is relatively large, we only consider the top 5,000 neighbors (MAP@5000), when computing MAP for NUS-WIDE, while for CIFAR-10 and MIRFlickr-25K, we calculate MAP for the entire retrieval database (MAP@ALL).

## 4.2. Implementation details

LabNet is built with four fully-connected layers, with which the input labels are transformed into hash codes ( $L \rightarrow 4096 \rightarrow 2048 \rightarrow N$ ). Here the output includes both the  $K$ -dimensional hash code and the  $C$ -dimensional multi-label predictions,  $N = K + C$ .

We built ImgNet based on Resnet50, the extracted visual features of Resnet are embedded into 2048-dimensional semantic features, which is followed by the two extra layers (i.e., Hash layer and Classification layer) with  $K$  nodes for hash code generation and  $C$  nodes for classification. It is noted that except for output layers, the network is pre-trained on ImageNet dataset.

The implementation of our method is based on the Pytorch framework and executed on NVIDIA TITAN X GPUs for 120 epoch-hs of training. The hyper-parameters in LabNet, set  $\alpha, \lambda, \eta, \beta$  are set to 2,0.5,0.5,0.1 respectively. The hyper-parameters in ImgNet,  $\alpha, \lambda, \gamma, \mu, \eta, \beta$  to 0.01,1,0.01,1,2 and 0.05 respectively. As can be observed from Fig.3, Labnet maintains a stable and robust retrieval performance under different choices of margin parameter, especially for small

margin parameters. Hence we simply set  $m$  to 0 for all the scenarios.

The Adam optimizer[20] is applied to LabNet, while the stochastic Gradient descent (SGD) method is applied to ImgNet. The batch size is set to 64. The learning rates are chosen from  $10^{-3}$  to  $10^{-8}$  with a momentum of 0.9.

## 4.3. Performance evaluation

### 4.3.1. Comparison to State of the Art

To validate the retrieval performance of our method, we compare the experimental results of SADH with other state-of-the-art methods including LSH [1], SH [7], ITQ [2], LFH [54], DSDH [40], HashNet [13], DPSH [10], DBDH [55], CSQ [56] and DSEH [41] on CIFAR-10, NUS-WIDE and MIRFlickr-25K. Table 1 shows the top 10 retrieved images in database for 3 sampled images in MIRFlickr-25K, it can be observed that in difficult cases, SADH reveals better semantic consistency than DSDH. Table 2 to Table 4 report the MAP results of different methods, note that for NUS-WIDE, MAP is calculated for the top 5000 returned neighbors. Fig.6-11 show the overall retrieval performance of SADH compared to other baselines in terms of precision-recall curve and precision curves by varying the number of top returned images, shown from 1 to 1000, on NUS-WIDE, CIFAR-10 and MIRFlickr-25K respectively. SADH substantially outperforms all other state-of-the-art methods. It can be noticed that SADH outperforms other methods for almost all the lengths of hash bits with a steady performance on both datasets. This is due to the multi-task learning structure in our method with which the classification output and hashing output are obtained independently, and the two tasks are not mutually interfered. It is also noteworthy that, with abundant semantic information leveraged from the self-supervised network and the pairwise information derived from the margin-scalable constraint, SADH obtained an impressive retrieval performance on both single-labeled CIFAR-10 and multi-labeled datasets (i.e., NUS-WIDE and MIRFlickr-25K).

### 4.3.2. Sensitivity to margin parameter

To demonstrate the earlier hypothesis of two networks' sensitivity to margin parameter in contrastive loss, we replace the scalable margin module in ImgNet by a constant margin  $m$  used in LabNet and report their MAP with 48-bit length under different choices of  $m$  on CIFAR-10 and MIRFlickr-25K. As shown in Fig. 3, we can see that under different choices of margin, LabNet reveals relatively slight changes in MAP, while ImgNet is highly sensitive to the choice of margin with the largest decrease of MAP score of roughly 0.14 when margin = 0 and margin = 0.2 on CIFAR-10. Which reveals the significance of properly selecting the margin value in deciding the retrieval performance of feature learning network.








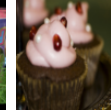










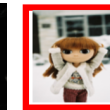

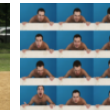




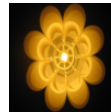

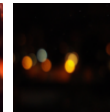
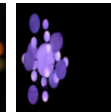
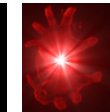
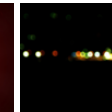
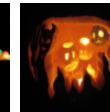

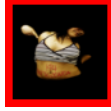


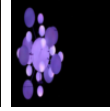
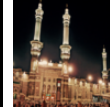
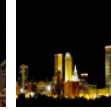
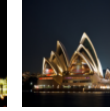






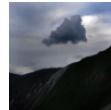
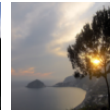
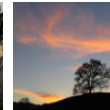
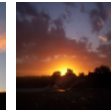
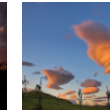

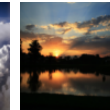









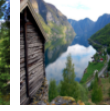
## 4.4. Empirical analysis

Three additional experimental settings are designed and used to further analyse SADH.



**Table 1**

Examples of top 10 retrieved images by SADH and DSDH on MIRFlickr-25K for 48 bits. The semantically incorrect images are marked with a red border.

Query	Top10 Retrieved Images										
	SADH										
	DSDH										
	SADH										
	DSDH										
	SADH										
	DSDH										

**Table 2**  
 MAP@ALL on CIFAR-10.

Method	CIFAR-10 (MAP@ALL)			
	16 bits	32 bits	48 bits	64 bits
LSH[1]	0.4443	0.5302	0.5839	0.6326
ITQ[2]	0.2094	0.2355	0.2424	0.2535
SH[7]	0.1866	0.1900	0.2044	0.2020
LFH[54]	0.1599	0.1608	0.1705	0.1693
DSDH[40]	0.7514	0.7579	0.7808	0.7690
HashNet[13]	0.6975	0.7821	0.8045	0.8128
DPSH[10]	0.7870	0.7807	0.7982	0.8003
DBDH[55]	0.7892	0.7803	0.7797	0.7914
CSQ[56]	0.7761	0.7775	-	0.7741
DSEH[41]	0.8025	0.8130	0.8214	0.8301
SADH	<b>0.8755</b>	<b>0.8832</b>	<b>0.8913</b>	<b>0.8783</b>

**Table 3**  
 MAP@5000 on NUS-WIDE.

Method	NUS-WIDE (MAP@5000)			
	16 bits	32 bits	48 bits	64 bits
LSH[1]	0.4443	0.5302	0.5839	0.6326
ITQ[2]	0.2094	0.2355	0.2424	0.2535
SH[7]	0.1866	0.1900	0.2044	0.2020
LFH[54]	0.1599	0.1608	0.1705	0.1693
DSDH[40]	0.7941	0.8076	0.8318	0.8297
HashNet[13]	0.7554	0.8163	0.8340	0.8439
DPSH[10]	0.8094	0.8325	0.8441	<b>0.8520</b>
DBDH[55]	0.8052	0.8107	0.8277	0.8324
CSQ[56]	0.7853	0.8213	-	0.8316
DSEH[41]	0.7319	0.7466	0.7602	0.7721
SADH	<b>0.8352</b>	<b>0.8454</b>	<b>0.8487</b>	0.8503

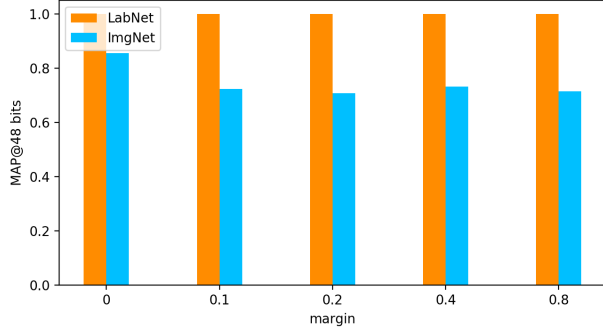
#### 4.4.1. Ablation study

We investigate the impact of the different proposed modules on the retrieval performance of SADH. SADH-asm refers

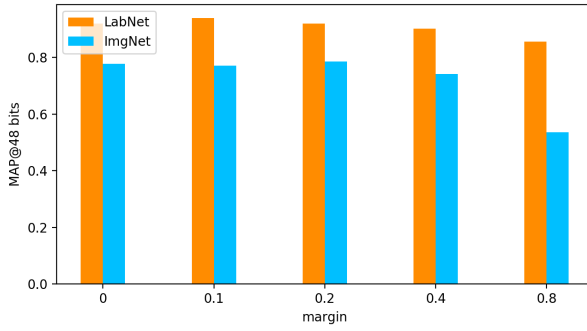
to ImgNet without asymmetric guidance from LabNet, SADH-mars is built by removing the margin-scalable constraint from ImgNet, SADH-cos refers to replacing the cosine similarity

**Table 4**  
MAP@ALL on MIRFLICKR-25K.

Method	MIRFlickr-25K (MAP@ALL)			
	16 bits	32 bits	48 bits	64 bits
DSDH[40]	0.7541	0.7574	0.7616	0.7680
HashNet[13]	0.7440	0.7685	0.7757	0.7815
DPSH[10]	0.7672	0.7694	0.7722	0.7772
DBDH[55]	0.7530	0.7615	0.7634	0.7653
CSQ[56]	0.6702	0.6735	-	0.6843
DSEH[41]	0.6832	0.6863	0.6974	0.6970
SADH	<b>0.7731</b>	<b>0.7698</b>	<b>0.7993</b>	<b>0.7873</b>



(a) CIFAR-10



(b) MIRFlickr-25K

**Figure 3:** Sensitivity analysis on the margin parameter

module in both ImgNet and LabNet by the logarithm Maximum a Posterior (MAP) estimation of pairwise similarity loss which is used in many deep hashing approaches [40, 41]:

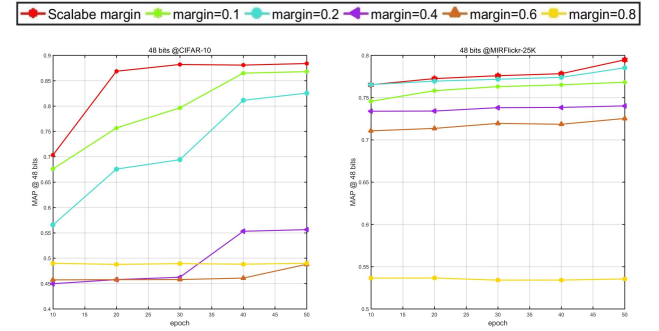
$$J_s = - \sum_{i,j=1}^m (S_{i,j} H_i^T H_j - \log(1 + \exp(H_i^T H_j))) \quad (12)$$

Results are shown on Table 2 for both NUS-WIDE and CIFAR-10 for hash codes of 32 bits. Considering the results, we can see that the asymmetric constraint with semantic information from LabNet plays an essential role on the performance of our method, meanwhile the margin-scalable constraint from ImgNet itself also significantly improves retrieval accuracy. It can also be observed that when using the cosine similarity, better performance is achieved than using the MAP estimation of pairwise similarity.

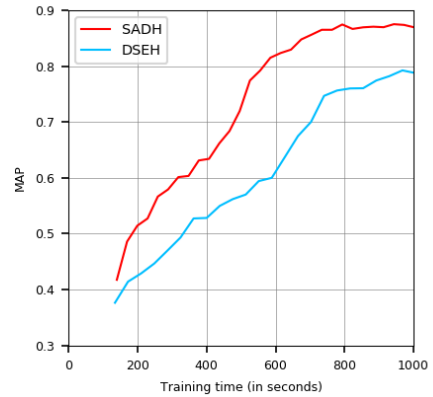
**Table 5**  
Ablation study on several modules in SADH, with MAP on NUS-WIDE and CIFAR-10 at hash length 32 bits

Methods	NUS-WIDE (MAP@5000)	CIFAR-10 (MAP@ALL)
SADH-asm	0.7115	0.7701
SADH-mars	0.8174	0.8249
SADH-cos	0.8168	0.8502
SADH	<b>0.8454</b>	<b>0.8832</b>

As a further demonstration of the effectiveness of the margin-scalable constraint, we compare it with several choices of single constants on our SADH. For 50 epochs, the top 5000 MAP results on MIR-Flickr25K and CIFAR-10 are given for every 10 epochs respectively. As illustrated in Fig.4. It is clear that in both the single-labeled and multi-labeled scenario, a scalable margin achieves better retrieval accuracy than using fixed margin constants. Furthermore, it is observed that on CIFAR-10, scalable margin result in faster convergence of SADH during training.



**Figure 4:** Map during 50 epochs on CIFAR-10 and MIRFlickr-25K with different choice of margins.



**Figure 5:** Training efficiency of SADH compared to DSEH on CIFAR-10.

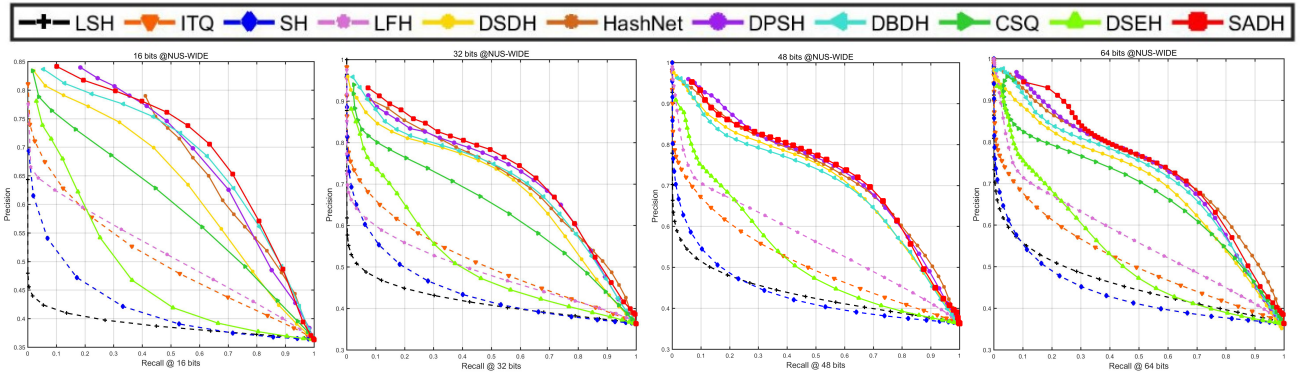


Figure 6: Precision-recall curves on NUS-WIDE.

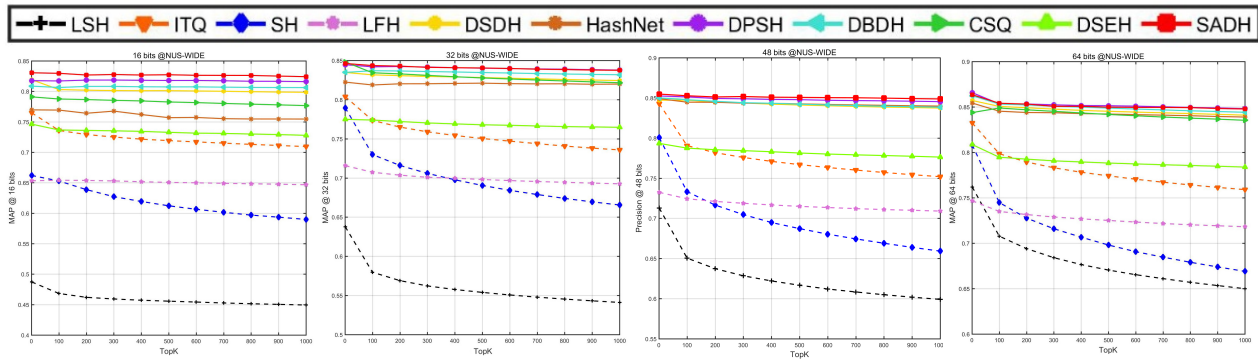


Figure 7: TopK-precision curves on NUS-WIDE.

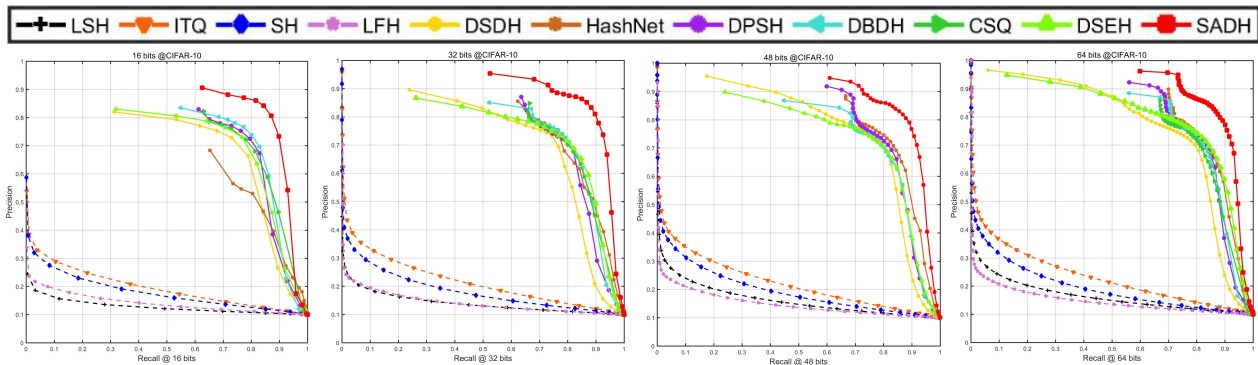


Figure 8: Precision-recall curves on CIFAR-10.

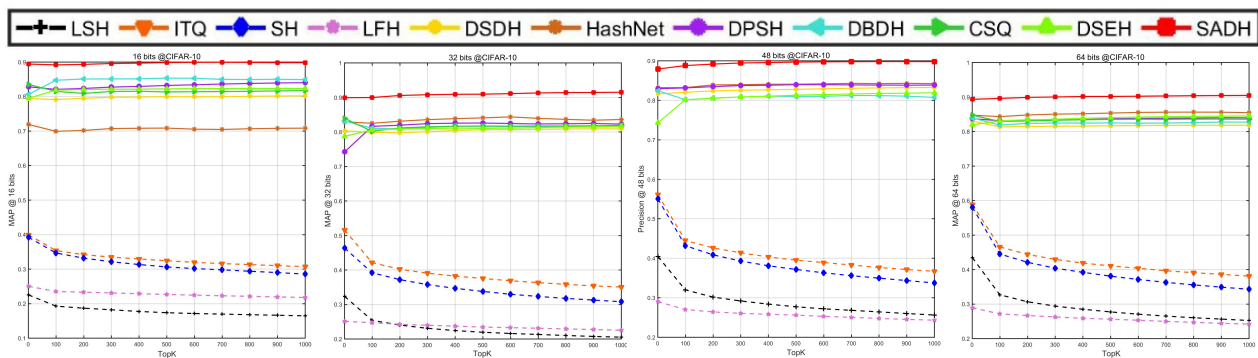


Figure 9: TopK-precision curves on CIFAR-10.

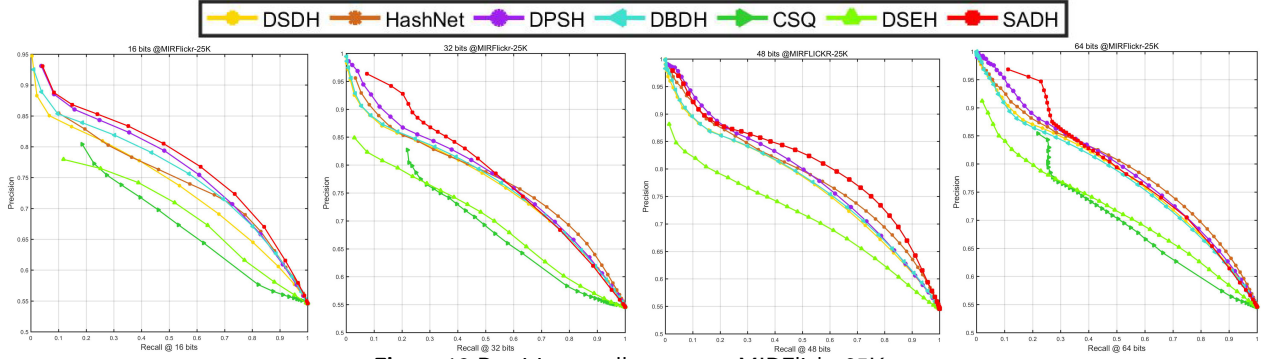


Figure 10: Precision-recall curves on MIRFlickr-25K.

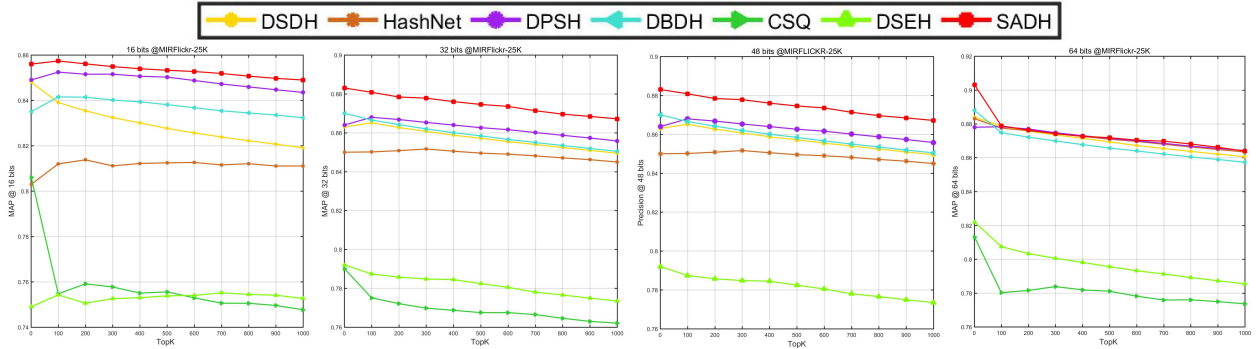


Figure 11: TopK-precision curves on MIRFlickr-25K.

#### 4.4.2. Training efficiency analysis

Fig 5 shows the change of MAP using 32-bit hash codes during training time of 1000 seconds, with a comparison of SADH and DSEH on CIFAR-10. We observe that SADH reduces training time by approximately two times to achieve a MAP of 0.6. Furthermore, SADH displays the tendency of convergence earlier than DSEH. SADH achieves a higher MAP than DSEH in less time. This is because ImgNet and LabNet are trained jointly for multiple rounds in DSEH, with the generated hash codes and semantic features of ImgNet being supervised by same number of those generated by LabNet. Whereas in SADH LabNet will cease to train after one round of convergence. And the converged LabNet will be utilized to produce hash code map and semantic feature map for each cases of semantic label. These maps directly supervise ImgNet with asymmetric pairwise correlation without further use of LabNet.

#### 4.4.3. Visualization of hash codes

Fig. 12 is the t-SNE [57] visualization of hash codes generated by DSDH and SADH on CIFAR-10, hash codes that belong to 10 different classes. Each class is assigned a different color. It can be observed that hash codes in different categories are discriminatively separated by SADH, while the hash codes generated by DSDH do not show such a clear characteristic. This is because the cosine similarity and scalable margin mechanism used in SADH can provide a more accurate inter-and-intra-class similarity preservation resulting in more discriminative hash codes in comparison to the mentioned form of pairwise similarity loss (12) used in DSDH.

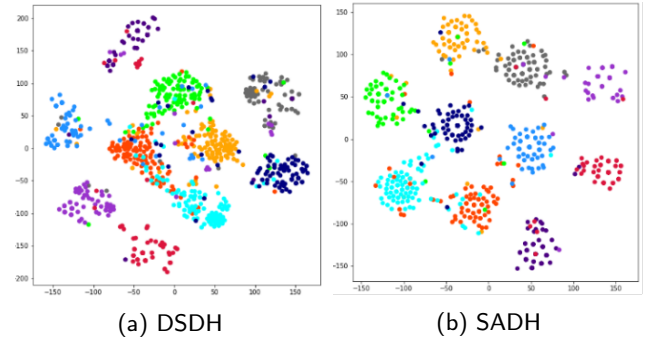
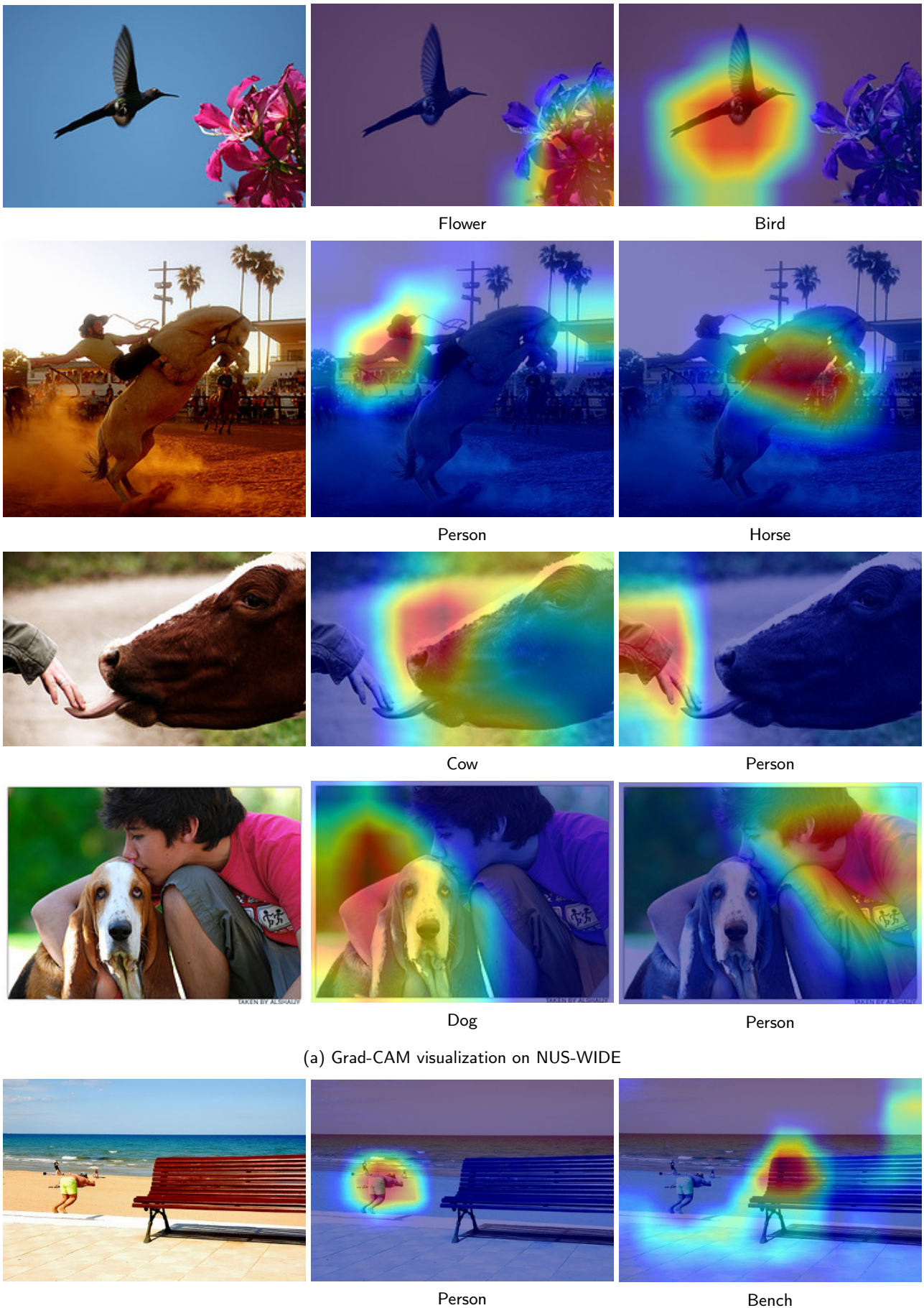


Figure 12: The t-SNE visualization of hash codes learned by DSDH and SADH.

#### 4.4.4. Heatmap visualization of focused regions

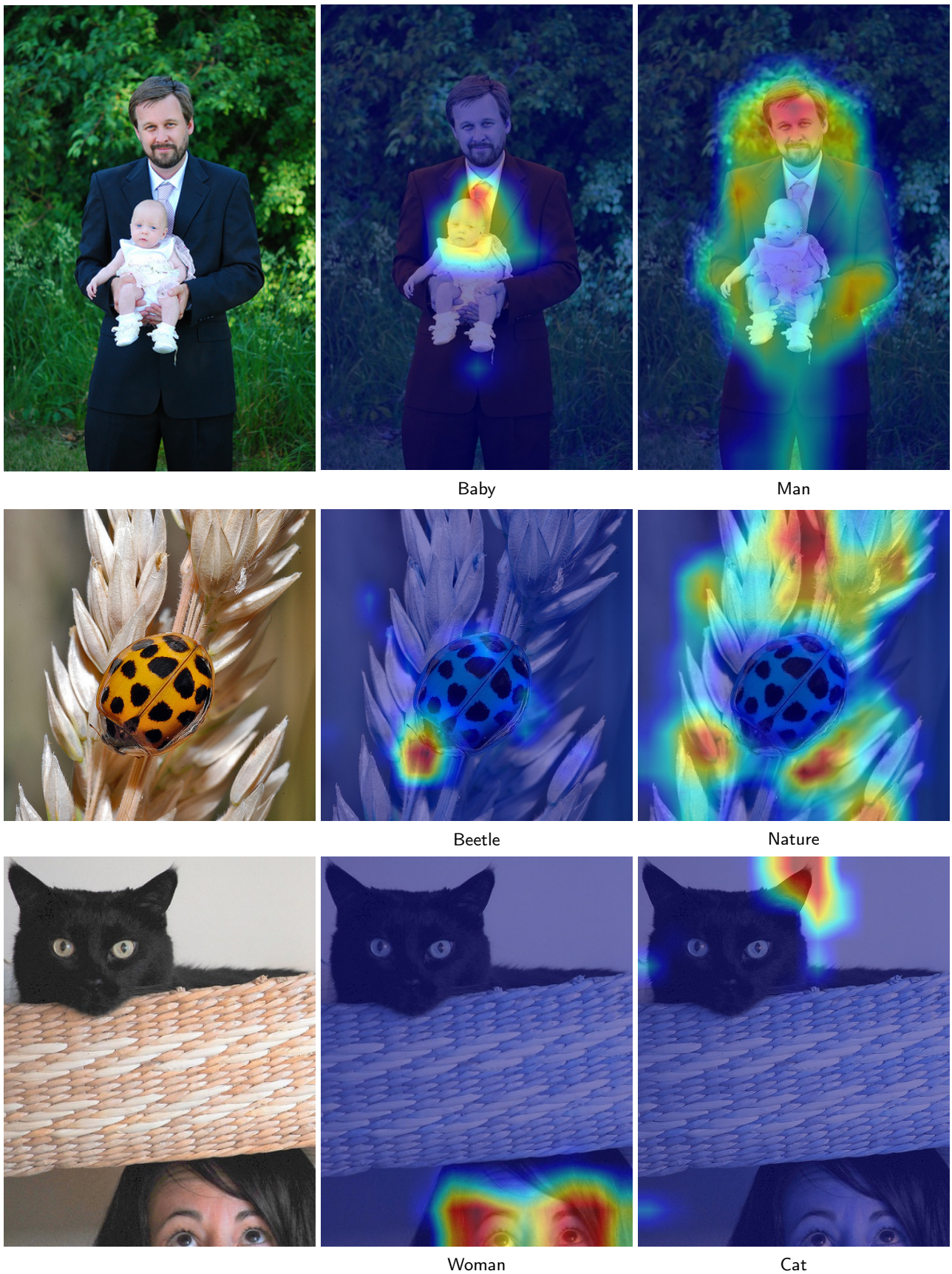
The Grad-CAM visualization of SADH following [58] for several sampled images on NUS-WIDE and MIR-Flickr25K is illustrated in Fig. 13. For each selected class of interest, Grad-CAM highlights the focused regions of convolutional feature maps. We observe that SADH accurately correlates selected semantics with corresponding regions, which is a strong proof for robust semantic feature preserving capacity of our SADH especially for multi-label scenarios.





(a) Grad-CAM visualization on NUS-WIDE





(b) Grad-CAM visualization on MIR-Flickr25K

**Figure 13:** Grad-CAM visualization of SADH for images sampled from multi-label benchmarks with respect to different ground-truth categories.

## 5. Conclusion

In this paper, we present a novel self-supervised asymmetric deep hashing method with a scalable constraint, namely SADH, for large-scale image retrieval. SADH includes two frameworks, one of which is LabNet, which extracts abundant semantic and pairwise information from semantic labels by a hash code map and semantic feature map, which in turn utilizes an efficiently asymmetric learning strategy to constrain the 2nd framework ImgNet, to generate hash codes with discrimination and well-preserved similarities. Additionally, the cosine similarity measurement and margin-scalable constraint are used to precisely-and-efficiently preserve similarity in the Hamming space. Comprehensive empirical evidence shows that SADH outperforms several state-of-the-art methods including traditional methods and deep hashing methods on three widely used benchmarks. In the future, we will explore to apply the proposed margin scalable constraint technique to other hash methods like cross-model hashing and real world applications like person re-identification.

## Acknowledgements

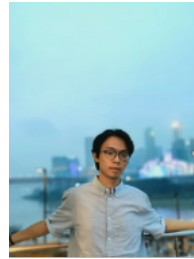
This work was supported by the [National Natural Science Foundation of China \(61806168\)](#), Fundamental Research Funds for the Central Universities (SWU117059), and Venture & Innovation Support Program for Chongqing Overseas Returnees (CX2018075).

## References

- [1] A. Gionis, P. Indyk, R. Motwani, et al., Similarity search in high dimensions via hashing, in: *Vldb*, volume 99, 1999, pp. 518–529.
- [2] Y. Gong, S. Lazebnik, A. Gordo, F. Perronnin, Iterative quantization: A procrustean approach to learning binary codes for large-scale image retrieval, *IEEE transactions on pattern analysis and machine intelligence* 35 (2012) 2916–2929.
- [3] J. Wang, H. T. Shen, J. Song, J. Ji, Hashing for similarity search: A survey, *CoRR* abs/1408.2927 (2014).
- [4] K. He, F. Wen, J. Sun, K-means hashing: An affinity-preserving quantization method for learning binary compact codes, in: *Proceedings of the IEEE conference on computer vision and pattern recognition*, 2013, pp. 2938–2945.
- [5] W. Liu, J. Wang, R. Ji, Y.-G. Jiang, S.-F. Chang, Supervised hashing with kernels, in: *2012 IEEE Conference on Computer Vision and Pattern Recognition*, IEEE, 2012, pp. 2074–2081.
- [6] B. Kulis, T. Darrell, Learning to hash with binary reconstructive embeddings, in: *Advances in neural information processing systems*, 2009, pp. 1042–1050.
- [7] Y. Weiss, A. Torralba, R. Fergus, Spectral hashing, *Advances in neural information processing systems* 21 (2008) 1753–1760.
- [8] M. Norouzi, D. J. Fleet, Minimal loss hashing for compact binary codes, in: *ICML*, 2011.
- [9] M. Norouzi, D. J. Fleet, R. R. Salakhutdinov, Hamming distance metric learning, in: *Advances in neural information processing systems*, 2012, pp. 1061–1069.
- [10] W.-J. Li, S. Wang, W.-C. Kang, Feature learning based deep supervised hashing with pairwise labels, *IJCAI* (2016) 1711–1717.
- [11] H. Lai, Y. Pan, Y. Liu, S. Yan, Simultaneous feature learning and hash coding with deep neural networks, in: *Proceedings of the IEEE conference on computer vision and pattern recognition*, 2015, pp. 3270–3278.
- [12] H. Zhu, M. Long, J. Wang, Y. Cao, Deep hashing network for efficient similarity retrieval, in: *Thirtieth AAAI Conference on Artificial Intelligence*, 2016.
- [13] Z. Cao, M. Long, J. Wang, P. S. Yu, Hashnet: Deep learning to hash by continuation, in: *Proceedings of the IEEE international conference on computer vision*, 2017, pp. 5608–5617.
- [14] Y. Cao, M. Long, B. Liu, J. Wang, Deep cauchy hashing for hamming space retrieval, in: *Proceedings of the IEEE Conference on Computer Vision and Pattern Recognition*, 2018, pp. 1229–1237.
- [15] B. Liu, Y. Cao, M. Long, J. Wang, J. Wang, Deep triplet quantization, in: *Proceedings of the 26th ACM international conference on Multimedia*, 2018, pp. 755–763.
- [16] T.-S. Chua, J. Tang, R. Hong, H. Li, Z. Luo, Y. Zheng, Nus-wide: a real-world web image database from national university of singapore, in: *Proceedings of the ACM international conference on image and video retrieval*, 2009, pp. 1–9.
- [17] M. J. Huiskes, M. S. Lew, The mir flickr retrieval evaluation, in: *Proceedings of the 1st ACM international conference on Multimedia information retrieval*, 2008, pp. 39–43.
- [18] M. A. Carreira-Perpinán, R. Razičperchikolaei, Hashing with binary autoencoders, in: *Proceedings of the IEEE conference on computer vision and pattern recognition*, 2015, pp. 557–566.
- [19] Q.-Y. Jiang, W.-J. Li, Asymmetric deep supervised hashing, *AAAI* (2018) 3342–3349.
- [20] D. P. Kingma, J. Ba, Adam: A method for stochastic optimization, *ICLR* (Poster) (2015).
- [21] X. Liu, J. He, B. Lang, S.-F. Chang, Hash bit selection: a unified solution for selection problems in hashing, in: *Proceedings of the IEEE conference on computer vision and pattern recognition*, 2013, pp. 1570–1577.
- [22] J. Wang, S. Kumar, S.-F. Chang, Semi-supervised hashing for large-scale search, *IEEE transactions on pattern analysis and machine intelligence* 34 (2012) 2393–2406.
- [23] F. Yu, S. Kumar, Y. Gong, S.-F. Chang, Circulant binary embedding, in: *International conference on machine learning*, 2014, pp. 946–954.
- [24] T. Yuan, W. Deng, J. Hu, Distortion minimization hashing, *IEEE Access* 5 (2017) 23425–23435.
- [25] K. He, X. Zhang, S. Ren, J. Sun, Deep residual learning for image recognition, in: *Proceedings of the IEEE conference on computer vision and pattern recognition*, 2016, pp. 770–778.
- [26] J. Wang, J. Wang, N. Yu, S. Li, Order preserving hashing for approximate nearest neighbor search, in: *Proceedings of the 21st ACM international conference on Multimedia*, 2013, pp. 133–142.
- [27] A. Krizhevsky, I. Sutskever, G. E. Hinton, Imagenet classification with deep convolutional neural networks, *Communications of the ACM* 60 (2017) 84–90.
- [28] J. Tang, Z. Li, X. Zhu, Supervised deep hashing for scalable face image retrieval, *Pattern Recognition* 75 (2018) 25–32.
- [29] Y. Guo, Y. Liu, A. Oerlemans, S. Lao, S. Wu, M. S. Lew, Deep learning for visual understanding: A review, *Neurocomputing* 187 (2016) 27–48.
- [30] H. Li, Z. Lin, X. Shen, J. Brandt, G. Hua, A convolutional neural network cascade for face detection, in: *Proceedings of the IEEE conference on computer vision and pattern recognition*, 2015, pp. 5325–5334.
- [31] Z. Liu, X. Li, P. Luo, C.-C. Loy, X. Tang, Semantic image segmentation via deep parsing network, in: *Proceedings of the IEEE international conference on computer vision*, 2015, pp. 1377–1385.
- [32] K. He, X. Zhang, S. Ren, J. Sun, Spatial pyramid pooling in deep convolutional networks for visual recognition, *IEEE transactions on pattern analysis and machine intelligence* 37 (2015) 1904–1916.
- [33] R. Girshick, Fast r-cnn, in: *Proceedings of the IEEE international conference on computer vision*, 2015, pp. 1440–1448.
- [34] S. Ren, K. He, R. Girshick, J. Sun, Faster r-cnn: Towards real-time object detection with region proposal networks, in: *Advances in neural information processing systems*, 2015, pp. 91–99.
- [35] S. Wu, A. Oerlemans, E. M. Bakker, M. S. Lew, Deep binary codes for large scale image retrieval, *Neurocomputing* 257 (2017) 5–15.



- Machine Learning and Signal Processing for Big Multimedia Analysis.
- [36] Y. Guo, Y. Liu, A. Oerlemans, S. Lao, S. Wu, M. S. Lew, Deep learning for visual understanding: A review, *Neurocomputing* 187 (2016) 27–48. Recent Developments on Deep Big Vision.
- [37] X. Wang, X. Zou, E. M. Bakker, S. Wu, Self-constraining and attention-based hashing network for bit-scalable cross-modal retrieval, *Neurocomputing* 400 (2020) 255–271.
- [38] R. Xia, Y. Pan, H. Lai, C. Liu, S. Yan, Supervised hashing for image retrieval via image representation learning., in: *AAAI*, volume 1, 2014, p. 2.
- [39] Q.-Y. Jiang, X. Cui, W.-J. Li, Deep discrete supervised hashing, *IEEE Transactions on Image Processing* 27 (2018) 5996–6009.
- [40] Q. Li, Z. Sun, R. He, T. Tan, A general framework for deep supervised discrete hashing, *International Journal of Computer Vision* 128 (2020) 2204–2222.
- [41] N. Li, C. Li, C. Deng, X. Liu, X. Gao, Deep joint semantic-embedding hashing., in: *IJCAI*, 2018, pp. 2397–2403.
- [42] Z. Yang, O. I. Raymond, W. Sun, J. Long, Asymmetric deep semantic quantization for image retrieval, *IEEE Access* 7 (2019) 72684–72695.
- [43] Z. Zhang, Z. Lai, Z. Huang, W. K. Wong, G.-S. Xie, L. Liu, L. Shao, Scalable supervised asymmetric hashing with semantic and latent factor embedding, *IEEE Transactions on Image Processing* 28 (2019) 4803–4818.
- [44] W. Gu, X. Gu, J. Gu, B. Li, Z. Xiong, W. Wang, Adversary guided asymmetric hashing for cross-modal retrieval, in: *Proceedings of the 2019 on International Conference on Multimedia Retrieval*, 2019, pp. 159–167.
- [45] X. Lu, Y. Chen, X. Li, Hierarchical recurrent neural hashing for image retrieval with hierarchical convolutional features, *IEEE transactions on image processing* 27 (2017) 106–120.
- [46] H. Liu, R. Wang, S. Shan, X. Chen, Deep supervised hashing for fast image retrieval, in: *Proceedings of the IEEE conference on computer vision and pattern recognition*, 2016, pp. 2064–2072.
- [47] H.-F. Yang, K. Lin, C.-S. Chen, Supervised learning of semantics-preserving hash via deep convolutional neural networks, *IEEE transactions on pattern analysis and machine intelligence* 40 (2017) 437–451.
- [48] T. Yao, F. Long, T. Mei, Y. Rui, Deep semantic-preserving and ranking-based hashing for image retrieval., in: *IJCAI*, volume 1, 2016, p. 4.
- [49] C. Li, C. Deng, N. Li, W. Liu, X. Gao, D. Tao, Self-supervised adversarial hashing networks for cross-modal retrieval, in: *Proceedings of the IEEE conference on computer vision and pattern recognition*, 2018, pp. 4242–4251.
- [50] Y. Chen, X. Lu, Deep discrete hashing with pairwise correlation learning, *Neurocomputing* 385 (2020) 111–121.
- [51] X. Wang, Y. Shi, K. M. Kitani, Deep supervised hashing with triplet labels, in: *Asian conference on computer vision*, Springer, 2016, pp. 70–84.
- [52] A. Krizhevsky, G. Hinton, et al., Learning multiple layers of features from tiny images (2009).
- [53] R. Zhang, L. Lin, R. Zhang, W. Zuo, L. Zhang, Bit-scalable deep hashing with regularized similarity learning for image retrieval and person re-identification, *IEEE Transactions on Image Processing* 24 (2015) 4766–4779.
- [54] P. Zhang, W. Zhang, W.-J. Li, M. Guo, Supervised hashing with latent factor models, in: *Proceedings of the 37th international ACM SIGIR conference on Research & development in information retrieval*, 2014, pp. 173–182.
- [55] X. Zheng, Y. Zhang, X. Lu, Deep balanced discrete hashing for image retrieval, *Neurocomputing* (2020).
- [56] L. Yuan, T. Wang, X. Zhang, F. E. Tay, Z. Jie, W. Liu, J. Feng, Central similarity quantization for efficient image and video retrieval, in: *Proceedings of the IEEE/CVF Conference on Computer Vision and Pattern Recognition*, 2020, pp. 3083–3092.
- [57] J. Donahue, Y. Jia, O. Vinyals, J. Hoffman, T. Darrell, Decaf: A deep convolutional activation feature for generic visual recognition (2013).
- [58] R. R. Selvaraju, M. Cogswell, A. Das, R. Vedantam, D. Parikh, D. Batra, Grad-cam: Visual explanations from deep networks via gradient-based localization, *International Journal of Computer Vision* 128 (2020) 336–359.



**Zhengyang Yu** received his B.S. degree in the College of Computer & Information Science, Southwest University. His current research interests include computer vision and pattern recognition, large-scale instance retrieval and person re-identification.



**Zhihao Dou** received his B.S degree in Automation in the College of Computer & Information Science, Southwest University in 2020. He works as an intern in State Grid Corporation of China. His research interests are computer version and data mining.



**Erwin M. Bakker** is co-director of the LIACS Media Lab at Leiden University. He has published widely in the fields of image retrieval, audio analysis and retrieval and bioinformatics. He was closely involved with the start of the International Conference on Image and Video Retrieval (CIVR) serving on the organizing committee in 2003 and 2005. Moreover, he regularly serves as a program committee member or organizing committee member for scientific multimedia and human-computer interaction conferences and workshops.



**Song Wu** received his B.S. degree and M.S. degree in Computer Science from the Southwest University, Chongqing, China, in 2009 and 2012, respectively. He received his Ph.D from the Leiden Institute of Advanced Computer Science (LIACS), Leiden University, Netherlands. He is a member of the Overseas High-level Talent Program in Chongqing and currently working at the College of Computer and Information Science of Southwest University. His current research interests include large-scale image retrieval and classification, big data technology and deep learning based computer vision (the co-author of the most cited paper of journal *Neurocomputing*: Deep learning for visual understanding: A review).